

A constant extension ensembles model of double-stranded chain molecules

Fei Liu,* Luru Dai, and Tao Xu

Institute of Theoretical Physics, The Chinese Academy of Sciences, P. O. Box 2735, Beijing 100080, China

Zhong-can Ou-Yang

*Institute of Theoretical Physics, The Chinese Academy of Sciences, P. O. Box 2735, Beijing 100080, China and
Center for Advanced Study, Tsinghua University, Beijing 100084, China*

(Dated: November 17, 2018)

Because the constant extension ensemble of single chain molecule is not always equivalent with constant force ensemble, a model of double-stranded conformations, as in RNA molecules and β -sheets in proteins, with fixed extension constraint is built in this paper. Based on polymer-graph theory and the self-avoiding walks, sequence dependence and excluded-volume interactions are explicitly taken into account. Using the model, we investigate force-extension curves, contact distributions and force-temperature curves at given extensions. We find that, for the same homogeneous chains, the force-extension curves are almost consistent with the extension-force curves in the conjugated force ensembles. Especially, the consistence depends on chain lengths. But the curves of the two ensembles are completely different from each other if sequences are considered. In addition, contact distributions of homogeneous sequence show that the double-stranded regions in hairpin conformations tend to locate at two sides of the chain. We contribute the unexpected phenomena to the nonuniformity of excluded-volume interactions of the region and two tails with different lengths. This tendency will disappear if the interactions are canceled. Finally, in constant extension ensemble, the force-flipping transitions conjugated with re-entering phenomena in constant force ensemble are observed in hairpin conformations, while they do not present in secondary structure conformations.

I. INTRODUCTION

In recent years, advances in manipulation techniques have made it possible to measure and characterize biological macromolecules at single-molecule level. By using devices such as optical and magnetic tweezers, atomic force microscopy, basic mechanical, physical and chemical properties of fundamental biological objects, e.g., proteins, nucleic acids, and molecular motors were obtained[1, 2, 3, 4, 5]. Special efforts have been devoted to mechanical properties of the nucleic acids, from elastic stretching experiments early[1] to recently unzipping double-stranded DNA (dsDNA), single-stranded DNA (ssDNA) or RNA[2, 6, 7]. Many useful insights can be obtained by analyzing the extension-force curves (EFCs) or force-extension curves (FECs) recorded in experiments, e.g., S-dsDNA structure found[1, 8] and the measurement for the proportion of G/C compared to A/T contents along dsDNA sequence[6].

On the theoretical side, a number of models have been built to interpret or simulate nucleic acid mechanical experimental data and phenomena. Elastic properties of stretched dsDNA were described by Marko and Siggia[9], and Zhou *et al.*[10]. Montanari and Mézard revealed that a second order phase transition exhibits as stretching ssDNA[11]. Lubensky and Nelson presented an extensive theoretical investigation of mechanical unzipping dsDNA[12]. Gerland *et al.* explored quantitatively how secondary structures determine outcome of FECs[13]. Although great efforts have been contributed to DNA mechanical problem, we note that little theoretical works concerned about constant extension ensembles of ssDNA or RNA[13], in which two ends separation \mathbf{r} of chain is fixed, and the average force is measured[6]. It is known for a time that in a traditional single polymer system, the constant force and the constant extension ensembles are equivalent in thermodynamic limit, though for finite systems inequivalence might be expected[14]. For nucleic acid, however, the situation becomes more complex since the presence of monomer interactions and the absence of self-averaging arising from sequences[12, 15]. To study such ensembles further, we will modify and extend the statistical model of double-stranded chain conformations developed by Chen and Dill[16, 17] to fixed extension scenario. To be different from previous theories[13], the extended model retains a relatively high degree of realism, which the sequence dependence and excluded-volume (EV) interactions are took into account explicitly. Experiments have shown that sequences change EFCs or FECs dramatically[2, 6, 7, 8]; while very recent stretching ssDNA experiment revealed the importance of EV interactions[18]. The interactions were neglected before. On the other hand, the model is more “microscopic”, i.e., entropy of chain is computed from the number of conformations

*liufei@itp.ac.cn

directly. As the first step, we restrict the model on two dimension (2d) lattice; and the extension is specified to be one component of the separation \mathbf{r} for simplicity. More general constant \mathbf{r} will be given in future work.

The organization of the paper is as follows. In Sec. II, the statistical model of double-stranded chain molecules is simply reviewed. In Sec. III, we extend two classes of conformations, hairpin and RNA-like secondary structure to constant extension cases, respectively. In Sec. IV, we first investigate how FECs of two classes of conformations are changed with temperature, chain length and sequence. To relate FECs with molecule structures, monomer-monomer contact probability distributions are then introduced. As an illustration, the distributions of simpler hairpin conformations are calculated. It is unexpected to find that hairpin contacts tend to form at two sides of chain. To explore the underlying reason, we introduce the Asymmetric Function (AF), and find that the interesting phenomena are the results of nonuniform EV interactions of double-stranded regions and two tails with different lengths in hairpin conformations. At last part of this section, force-temperature curves (FTCs) at fixed extensions for homogeneous double-stranded chains are computed. This study comes from re-entering transitions observed in constant force ensembles[19, 20]. Force flipping phenomena are observed in hairpin conformations, but do not present in secondary structure. The “flipping” here is defined that when temperature decreases, force value first decreases and then increases; it finally decreases again as temperature is lower than some value. We believe that the phenomena in constant extension ensembles are conjugated with re-entering transition. Section V is our conclusion. The calculation of extensions with a special case in hairpin conformations is relegated in Appendix A.

II. THE DOUBLE-STRANDED CHAIN MODEL

The details of the statistical model of double-stranded chain molecules can be found in Refs. [16] and [17]. Here we just give a brief review.

A. Polymer graph theory

The model is based on polymer graphs, diagrammatic representations of the self-contacts made by different chain conformations. Fig. 1 shows a hairpin conformation and corresponding polymer graph: vertices represent the chain monomers, straight line links symbolize the covalent bonds, and curved links stand for spatial contact between monomers. A given polymer graph represents an ensemble of chain conformations that are consistent with given

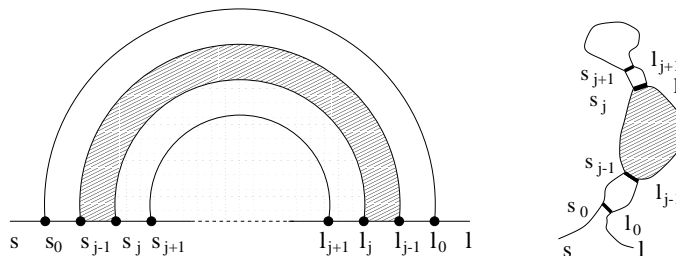


FIG. 1: The polymer graph of hairpin conformations. The shadowed region is a face of the graph. The graph is divided into two parts: two tails $[s, s_0]$ and $[l_0, l]$, and one double-stranded region, or CG enclosed by outmost link (s_0, l_0) . Here s and l are two end monomers in chain. The double-stranded region is composed of links nested each other: $(s_0, l_0), \dots, (s_{j-1}, l_{j-1}), (s_j, l_j), (s_{j+1}, l_{j+1})$.

contacts. Conformations having contacts other than those specified by the polymer graph belong to other graphs. In general, fewer curved links exist in a graph, a more larger number of chain conformations are consist with this graph. Any two pairs of curved links in a polymer graph must bear one of three relationships: nested, unrelated and crossing linked. Graphs of the double-stranded chain conformations involve no crossing links, examples of which include the simplest hairpin structure, such as dsDNA, and mainly secondary structures among nucleic acids and antiparallel β -sheets in proteins. In terms of polymer graph, the partition function of a $(N + 1)$ monomers $((N+1)$ -mer) chain molecule is given as a sum over all possible polymer graphs,

$$\mathcal{Q}_N(T) = \sum_{\Gamma} \Omega(\Gamma) e^{-E(\Gamma)/k_B T}, \quad (1)$$

where k_B is Boltzmann constant, T is temperature, Γ is an index of a possible polymer graph, $E(\Gamma)$ and $\Omega(\Gamma)$ are the energy and the number of conformations of the given polymer graph Γ , respectively. To calculate $\Omega(\Gamma)$, Chen and Dill developed a matrix multiplication method[16, 17].

B. The matrix method for a given polymer graph

A complex polymer graph can be divided into a series of faces consecutively, in which face is a region in graph that is bounded by curved and straight lines and contains no other edges; see the shadowed region in Fig. 1. Faces are classified into five types: left (L), middle (M), right (R), left-right (LR) and isolated (I), according to the arrangement of the nested curved links that bound the face. The calculation of the full partition function $\Omega(\Gamma)$ for a given graph Γ is correspondingly separated into two steps: to count all conformations for each face, as if they are isolated and independent of each other, and to assemble these conformations into $\Omega(\Gamma)$. To avoid that conformations of different faces bump into each other (EV interaction), more detailed information about the conformations of faces is needed. On two dimension (2D) lattice, it is realized by exact enumeration. First, conformations of each face are classified into sixteen types according to the shape of ports (inlet and outlet) through which it is connected to other faces. The shapes of ports are shown in Fig. 2. Then the compatibility between neighboring faces can be checked exactly through the spatial compatibility between the outlet of one face and the inlet of next face. It is convenient to introduce two matrices: the Face Count Matrix (FCM) \mathbf{S}_t , which matrix element $(\mathbf{S}_t)_{ij}$ is the number of conformations having an inlet conformation of type i ($1 \leq i \leq 4$) and an outlet conformation of type j ($1 \leq j \leq 4$) for a type t face, and viability matrix $\mathbf{Y}_{t_1 t_2}$, which element $(\mathbf{Y}_{t_1 t_2})_{ij}$ is 1 or 0 if connection of type i outlet of a type t_1 face and type j inlet of a type t_2 face is viable or not viable. For a hairpin graph Γ having M faces, $\Omega(\Gamma)$ is derived as a product of matrices:

$$\Omega(\Gamma) = \mathbf{U} \cdot \mathbf{S}_{t_M} \cdot \mathbf{Y}_{t_M t_{M-1}} \cdot \mathbf{S}_{t_{M-1}} \cdots \mathbf{S}_{t_1} \cdot \mathbf{U}^t, \quad (2)$$

where $\mathbf{U} = \{1, 1, 1, 1\}$, \mathbf{U}^t is the transpose of \mathbf{U} .

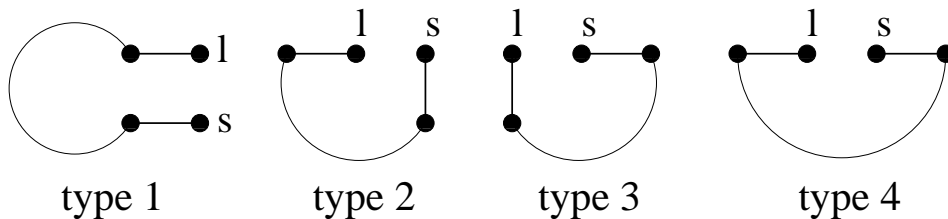


FIG. 2: The four types of port (inlet or outlet) shapes on 2D lattice.

C. The partition function

In order to calculate the partition function of a whole chain using Eq. 1, the sum over all possible polymer graphs is necessary. For the double-stranded conformations, an efficient dynamic programming algorithm was developed in Ref. [17]. The idea is to start with a short chain segment and elongate the segment by adding one monomer for each step, and to calculate recursively the partition function of the longer segment using the result of the shorter one. The algorithms will be discussed as needed in following sections. More useful alternative expression of Eq. 1 is

$$\mathcal{Q}_N(T) = \sum_E g_N(E) e^{-E/k_B T}, \quad (3)$$

where $g_N(E)$ is the density of states, or the number of conformations having energy E , which is defined as

$$g_N(E) = \sum_{\Gamma} \Omega(\Gamma) |_{E(\Gamma)=E}. \quad (4)$$

III. CONSTANT EXTENSION ENSEMBLES FOR DOUBLE-STRANDED CHAIN MOLECULES: HAIRPIN AND SECONDARY STRUCTURE CONFORMATIONS

Fig. 3 depicts the situation studied in this paper. Two ends of chain molecule are grasped by two pins. Instead of fixing end-to-end distance (EED) \mathbf{r} , its projection along direction \mathbf{x}_o , or extension x is required to be constant. Average force f along \mathbf{x}_o is recorded as a function of x . Because of extension constraint, the partition function Eq. 3 is modified to $\mathcal{Q}_N(x; T)$

$$\mathcal{Q}_N(T; x) = \sum_E g_N(E; x) e^{-\beta E}, \quad (5)$$

where $g_N(E; x)$ is the number of conformations whose extensions are x . Then force f can be calculated by

$$f(x, T) = -k_B T \frac{\partial}{\partial x} \log \mathcal{Q}_N(x; T). \quad (6)$$

Considering that our chain model is on 2D lattice, in following sections constant extension x is to be replaced by a discrete variable Δ .

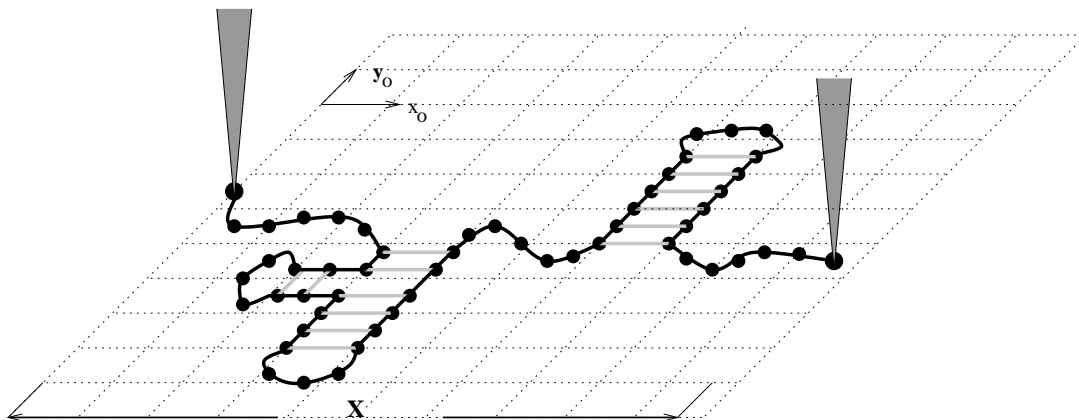


FIG. 3: Sketch of the constant extension experiment on the 2D lattice. The larger dark points represent two ends of a chain molecule; they are grasped by two pins. Monomers are denoted to be small dark points. In present paper, only projection component x of separation \mathbf{r} along direction \mathbf{x}_o is fixed as constant. Average force f along \mathbf{x}_o is recorded as a function of x .

The appearance of parameter, extension Δ requires the statistical model of double-stranded chains to be modified and extended carefully. In the next two sections, we will show how to compute $g_N(E; \Delta)$ of hairpin and secondary structure conformations, respectively.

A. Constant extension ensembles of hairpin conformations

As one of the simplest elements in secondary structure, hairpin conformations exist in a large class of biomolecules, such as RNA hairpin, peptide β -hairpin and DNA hairpin. Recent works showed that the hairpin conformations have remarkable thermodynamic and kinetic behaviors[17, 21]. In constant force ensembles, the mechanical behaviors of the hairpin conformations are completely different from that of secondary structure conformations[22]. It is interesting to see whether there is new difference presented in constant extension ensembles. In addition, more precise formula and the essence of theory for complex secondary structure conformations make us to explore their properties independently.

The polymer graphs of hairpin conformations are that every curved link bears a nested relationship with respect to every other curved link. The polymer graph is composed of two parts: two non-self-contacting tail chains (s, s_0) and (l_0, l) and one double-stranded region (s_0, l_0) , which is defined as Closed Graph (CG)[17]; see Fig. 1. The number of conformations for a given graph equals a multiplication of the number of double-stranded conformations and the number of two tails conformations. In terms of four types of the outermost faces, the graphs are classified into four types. (LR type is excluded from hairpin conformations). To sum over all polymer graphs, two matrices, the Closed Graph Count Matrix (CGCM), $\mathbf{G}^*_t [E, s_0, l_0]$ and diagonal matrix $\omega [s, s_0; l_0, l]$ have been defined: $(\mathbf{G}^*_t [E, s_0, l_0])_{ij}$ is the sum over the number of conformations for all possible t type graphs having energy E , given that the outermost link

spans from vertex l_0 to vertex s_0 and innermost and outermost links are in i and j types conformations; diagonal matrix element $(\omega[s, s_0; l_0, l])_{ii}$ is the number of conformations of two tails (s, s_0) and (l_0, l) that are spatially compatible with type i conformations. State density $g_N(E)$ then can be written as:

$$g_N(E) = \mathbf{U} \cdot \sum_{s_0, l_0, t} \omega[s, s_0; l_0, l] \cdot \mathbf{G}^*_t[E, s_0, l_0] \cdot \mathbf{U}^t, \quad (7)$$

here $1 \leq t \leq 4$ [17].

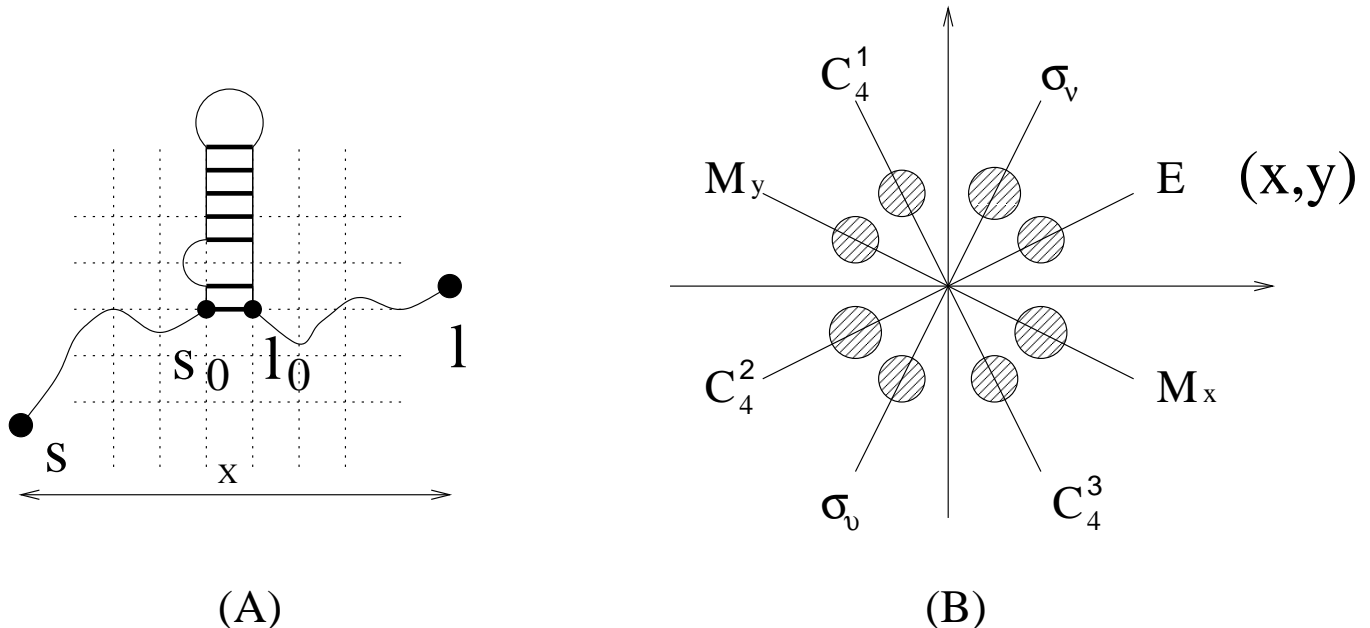


FIG. 4: (A) Sketch of hairpin conformations at constant extension x . Here the double-stranded region contributes $+1$ to extension of whole chain. (B) Illustration of how the conformation ended at (x, y) is distributed to whole lattice plane by eight square symmetric transformations, where the shadowed circles represent the double-stranded regions.

When the extension of hairpin conformations is fixed, $g_N(E)$ is then extended to $g_N(E, \Delta)$, and $\omega[s, s_0; l_0, l]$ is *nondegenerated* into $\omega[s, s_0; l_0, l|\Delta]$. We rewrite Eq. 7 as

$$g_N(E; \Delta) = \mathbf{U} \cdot \sum_{s_0, l_0, t} \omega[s, s_0; l_0, l|\Delta] \cdot \mathbf{G}^*_t[E, s_0, l_0] \cdot \mathbf{U}^t. \quad (8)$$

Fig. 4(a) shows that extensions of chain on 2D lattice do not involve any detailed CG structure directly, i.e., only the outmost link (s_0, l_0) contributes ± 1 or 0 to Δ . Though, in real nucleic acid, a typical distance of a hydrogen bond is about 3 times than the nucleotide distance, it does not make sense for our description on a coarse-grained level. Δ is enumerated with three steps: first, to fix one conformation of a given CG on lattice and grow two tails which are compatible with the graph type; then, to enumerate two tails extensions and combine them with distance of the graph according \mathbf{x}_o direction; finally, to distribute the conformation to full lattice plane by eight square symmetry transformations (D_4 group); see Fig. 4(b). The basic idea is very simple, however, it is very cumbersome to complete this process. Rather than to give a detailed analysis here, the process is illustrated in Appendix A by the simplest case.

Although the enumeration method gives quite accurate hairpin extensions, unfortunately, it is impossible to count longer chain. We propose a more practical approximation in the next section.

B. Constant extension ensembles of secondary structure conformations

Secondary structure can be seen as a tree-like structure into which four basic structure elements, helix, loops, bulges and junctions compose through self-similarity arrangement. Each graph of secondary structure conformations

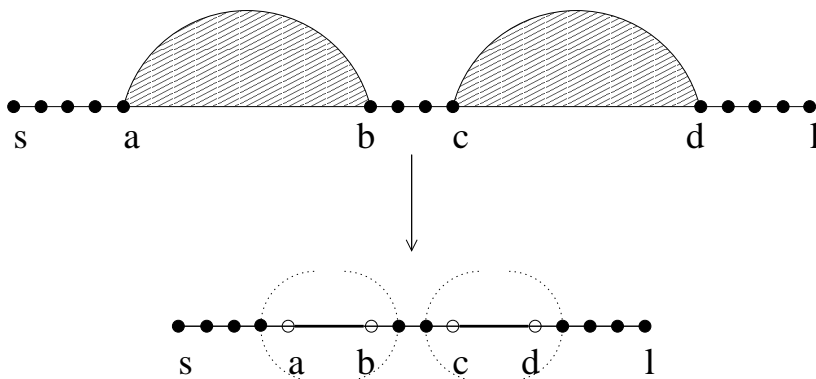


FIG. 5: Illustration of how unrelated closed polymer graphs are reduced into effective chain to calculate the number of conformations with fixed extensions. For example, two closed graphs $[a, b]$ and $[c, d]$ in upper are replaced by two bonds in below, and length of the effective chain is reduced to $(a - s) + (c - b) + (l - d) + 2$ from $l - s$. Considering that EV interactions of CGs and single-strand parts make conformations of the neighboring monomers of CGs to be “frozen”, it may be reasonable to reduce chain length more, showing here by dashed brackets. In present paper, the simplest case is considered.

is divided into two levels: the first lever is a combination of unrelated double-stranded regions connected with single-stranded chains; the second level is that each CG may be viewed as an independent secondary structure except that two end monomers of the region contact. We first simply review how to calculate the state density $g(E)$ without mechanical constraint. The necessary definitions are introduced.

To be different from hairpin conformations, the calculation of full state density of the secondary structure is more complex. First all possible CGCMs, $\mathbf{G}_t^*[E, a, b]$ (Note that LR-type faces are included) are computed, where (a, b) is the outmost link of the CG. Any CG is composed of smaller unrelated subclosed graphs, auxiliary matrices, $\mathbf{K}_t[E, l, a, b]$ counting a combination of conformations of all subgraphs are introduced, where *cyclelength* l is the total number of monomers of the single-stranded chains in $[a, b]$ [17]. CGCMs can be obtained by multiplication of matrix $\mathbf{K}_t[E, l, a, b]$ and the number of conformations of the single-stranded part. Then in order to combine conformations of unrelated graphs into whole, matrices $\mathbf{G}_t[E, s, a]$ having energy E for full polymer graph $[s, a]$ are defined, where $t = 0, 1, 2$ represent three full graph types which are classified depending on whether 0, 1 and 2 existing links are connected to the rightmost monomer, see Fig. 6. Their element $(\mathbf{G}_t[E, s, a])_{ij}$ is the number of conformations for graphs in which the outmost link (of rightmost subgraph) and the innermost link (of the leftmost subgraph) are in j and i conformations, respectively. All matrices mentioned above are calculated by dynamics programming algorithm[17]. The full density of states of the secondary structure conformations is written as [17]

$$g_N(E) = \mathbf{U} \cdot \sum_{t=0}^2 \mathbf{G}_t[E, s, l] \cdot \mathbf{U}^t. \quad (9)$$

Consider the number of conformations with fixed extension Δ . Because that the detailed structures of CGs do not affect the whole extensions directly as in hairpin case, CGs are viewed as *effective* covalent bonds connecting left and right parts of a chain; the effective bonds bear the EV interaction of CGs with other units in the chain. Thus the secondary structure conformations are identified to be “open” self-avoiding walks (OSAWs) with reduced monomers; see Fig. 5. OSAWs are self-avoid walks involving no neighboring contacts[17, 22]. The number of OSAWs whose extensions are Δ can be computed by enumeration and extrapolation method[22]. Although the effective chain approach (ECA) may overestimate the number of conformations for partially counting EV interactions, we think that it is valuable before better methods are found.

To realize the ECA, we modify the matrices $\mathbf{G}_t[E, s, a]$ to $\mathbf{G}_t[E, n, s, a]$, where new parameter n is the number monomers of the effective chain. The recursive relations in Ref. [17] (also see Fig. 6) are extended into following

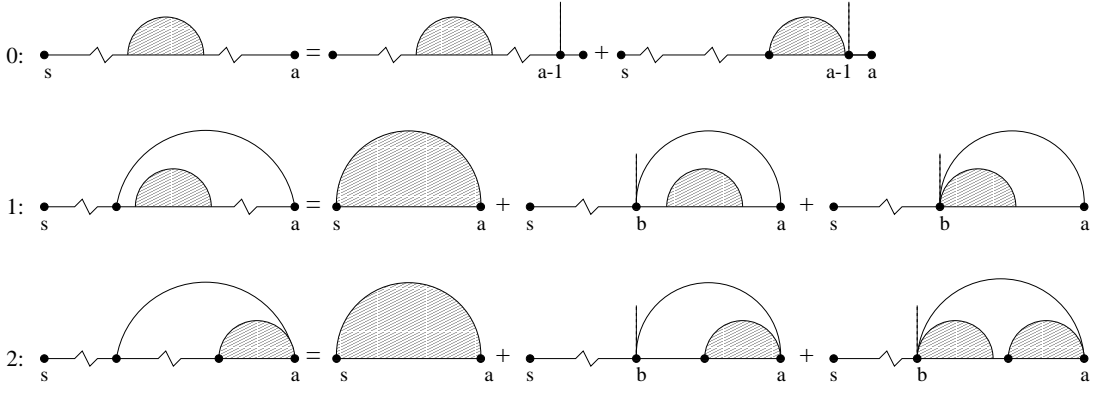


FIG. 6: the recursive relations for matrices $\mathbf{G}_t[E, n, s, a]$, where $t = 0, 1, 2$.

relations:

$$\mathbf{G}_0[E, n, s, a] = \mathbf{G}_0[E, n-1, s, a-1] + \mathbf{G}_1[E, n-1, s, a-1], \quad (10)$$

$$\begin{aligned} \mathbf{G}_1[E, n, s, a] &= \delta_{n,1} \sum_{t=L,M,I} \mathbf{G}^*_t[E, s, a] \\ &+ \sum_{0 < b < a} \sum_{E_1} \mathbf{G}_0[E - E_1, n-1, s, b] \sum_{t=L,M,I} \mathbf{G}^*_t[E_1, b, a] \\ &+ \sum_{0 < b < a} \sum_{E_1} \mathbf{G}_1[E - E_1, n-1, s, b] \sum_{t=M,I} \mathbf{G}^*_t[E_1, b, a], \end{aligned} \quad (11)$$

$$\begin{aligned} \mathbf{G}_2[E, n, s, a] &= \delta_{n,1} \sum_{t=R,LR} \mathbf{G}^*_t[E, s, a] \\ &+ \sum_{0 < b < a} \sum_{E_1} \mathbf{G}_0[E - E_1, n-1, s, b] \sum_{t=R,LR} \mathbf{G}^*_t[E_1, b, a] \\ &+ \sum_{0 < b < a} \sum_{E_1} \mathbf{G}_1[E - E_1, n-1, s, b] \mathbf{G}^*_R[E_1, b, a]. \end{aligned} \quad (12)$$

Correspondingly, $g_N(E)$ is extended to $g_N(E; \Delta)$ as

$$g_N(E; \Delta) = \sum_{n=1}^N C_x(n; \Delta) \sum_{t=0}^2 \mathbf{U} \cdot \mathbf{G}_t[E, n, s, l] \cdot \mathbf{U}^t \quad (13)$$

where $C_x(n; \Delta)$ is the number of conformations of n -step OSAWs whose final x coordinates are Δ . Eq. 13 clearly separates contribution of the unrelated CGs from the single-stranded parts.

Because the hairpin is one of four elements in secondary structure case, ECA should be suitable to it. We also note that exact enumeration still is available when the lengths of two tails are smaller than some value (27 in this paper), a mixture of two methods is applied in hairpin case. It is reasonable, for as the CG size is so large, or tails are so short that tail conformations are almost “frozen”, enumeration method is accurate. As the lengths of tails are relatively longer than CG size, or the EV interactions of CG and tail are smaller, the ECA may be available.

IV. TESTS OF THE MODEL: FECS, CONTACT DISTRIBUTIONS AND FORCE FLIPPING PHENOMENA

We have described how to extend the statistical mechanical model of double-stranded chain molecules to constant extension ensembles in previous sections. In this section, the model will be used to explore FECS, contact distribution, and force flipping phenomena. To account for specific monomer sequences, sequences are divided into two classes: homogeneous and RNA-like chain. Each contact of the homogeneous chain contributes one sticking energy $-\varepsilon$ ($\varepsilon < 0$). While RNA-like chain has a specific sequence of four types of monomers: A, U, C and G, resembling the 4 types of

bases of an RNA; only A-U pair or C-G pair contributes one sticking energy $-\varepsilon$. In following, we take the lattice spacing b .

But before beginning with our discussion, the even-odd oscillations in partition function $\mathcal{Q}_N(T; \Delta)$ with Δ have to be canceled, which are the results of 2D lattice restriction[23]. We damp the oscillations out simply by forming square root means of partition function as

$$\mathcal{Z}_N(T; \Delta) = [\mathcal{Q}_N(T; \Delta) * \mathcal{Q}_N(T; \Delta + 1)]^{1/2}. \quad (14)$$

$\mathcal{Q}_N(T; \Delta)$ in Eq. 6 then is replaced by $\mathcal{Z}_N(T; \Delta)$.

A. Force-Extension curves

We investigate how temperature T and monomer number $(N + 1)$ affect FECs of homogeneous chains of hairpin and secondary structure conformations, respectively; see Figs. 7. Here only positive extensions are given. There are common features in these FECs. First, forces f always monotonously increases as extensions x increase except the start part. Second, the FECs shapes in monotonous regions of any type of conformations are very similar at different N value, i.e., f may be the function of x/N , or relative extension $\rho = x/N$. Finally, at the same extension interval, the force changes are faster at higher temperature. To check the relationship of force and relative extension ρ , FECs of different N values at the same temperature are plotted together in terms of f versus ρ . We find that these FECs quickly tend to asymptotic curves as N increases; these curves are related only with temperature and chain conformation type (results are not shown in this paper). Differences in FECs between two classes conformations are also apparent: FECs of hairpin cases are identical over a longer region of extension than those of secondary structure conformations; when extensions increase, forces increase continuously and smoothly in secondary structure cases, while forces in hairpin cases are almost invariant, until dramatical jumps happened as extensions reaching their full length.

Comparing FECs with EFCs of homogeneous double-stranded chain molecules is valuable. The latter have been computed in Ref. [22] (see Fig. 8 therein). It is about equivalence of the two conjugated ensembles: the constant extension and the constant force[12, 14]. We find the FECs and EFCs of two ensembles are almost consistent in the monotonous regions, though small differences present. The deviation could be expected due to finite N -value[14].

To illustrate effects of specific monomer sequence, FECs of RNA sequences P5ab, P5abc Δ A, and P5abc are computed; see Fig. 8(a). These sequences come from force unfolding RNA experiments studied by Liphardt *et al.* recently[7]. To be very different from FECs of homogeneous chains, the FECs of heterogeneous chains are no longer increase monotonously: sawtooth-like oscillations present in all sequences. The force behaviors are very similar with the force curves observed in unzipping dsDNA experiments[6]. The complex features disappear at higher temperature, such as at $0.64\varepsilon/k_B$. We also compare the FECs with the EFCs of force stretched the same RNA sequence[22]: no oscillations was observed in constant force ensembles. Unlike the homogeneous chains, the equivalence of two conjugated ensembles is not guaranteed as consideration sequence effects. In particular, the force non-monotonicity even survives in thermodynamic limit for each sequence realization since the absence of self-averaging in biomolecules[15].

We also calculate FECs of random, alternating and designed sequences; see Fig. 8(b). The designed is composed of four elements, A, U, C and G arranged by $A \cdots ACCCCU \cdots UC \cdots CAAAAG \cdots G$, where the dots represent 15-mer A, U, C and G consecutively. Comparing the FECs of the artificial sequences with curves got before, we find the force curves of the random sequence is similar with the curves of biomolecular sequences in Fig. 8(a); the forces of the alternating sequence are almost the same with the results of homogeneous secondary structure chain; while the FEC of the designed sequence presents large force reduction at extension about a half of full length. From designed sequence arrangement, if no extension constraint, the molecule tends to form two independent identical hairpins simultaneously. The larger force reduction reflects completely collapsing of one hairpin. Interestingly, when force stretching the designed sequence, only one jump exhibits since higher cooperativity between two hairpins[22].

B. Contact distribution and asymmetric function

In order to gain insights into the molecular structure at any extension, we compute contact distribution $p(i, j; T, m)$ for every possible contact pair (i, j) , where m is the discrete value of extension. $p(i, j; T, m)$ is determined by the ratio of the conditional partition function $\mathcal{Z}_N(i, j; T, m)$ for all the conformations that contain contact (i, j) and full partition function $\mathcal{Z}_N(T, m)$, i.e., $p(i, j; T, m) = \mathcal{Z}_N(i, j; T, m) / \mathcal{Z}_N(T, m)$. As an example, the density diagrams of a 70-mer homogeneous hairpin chain at different extensions are shown in Fig. 9.

It is unexpected that nonzero contacts populate symmetrically two sides of the catercorner of diagrams when extensions are smaller, such as in Figs. 9(b) and (c). It means that the CG regions in hairpin conformations tend to

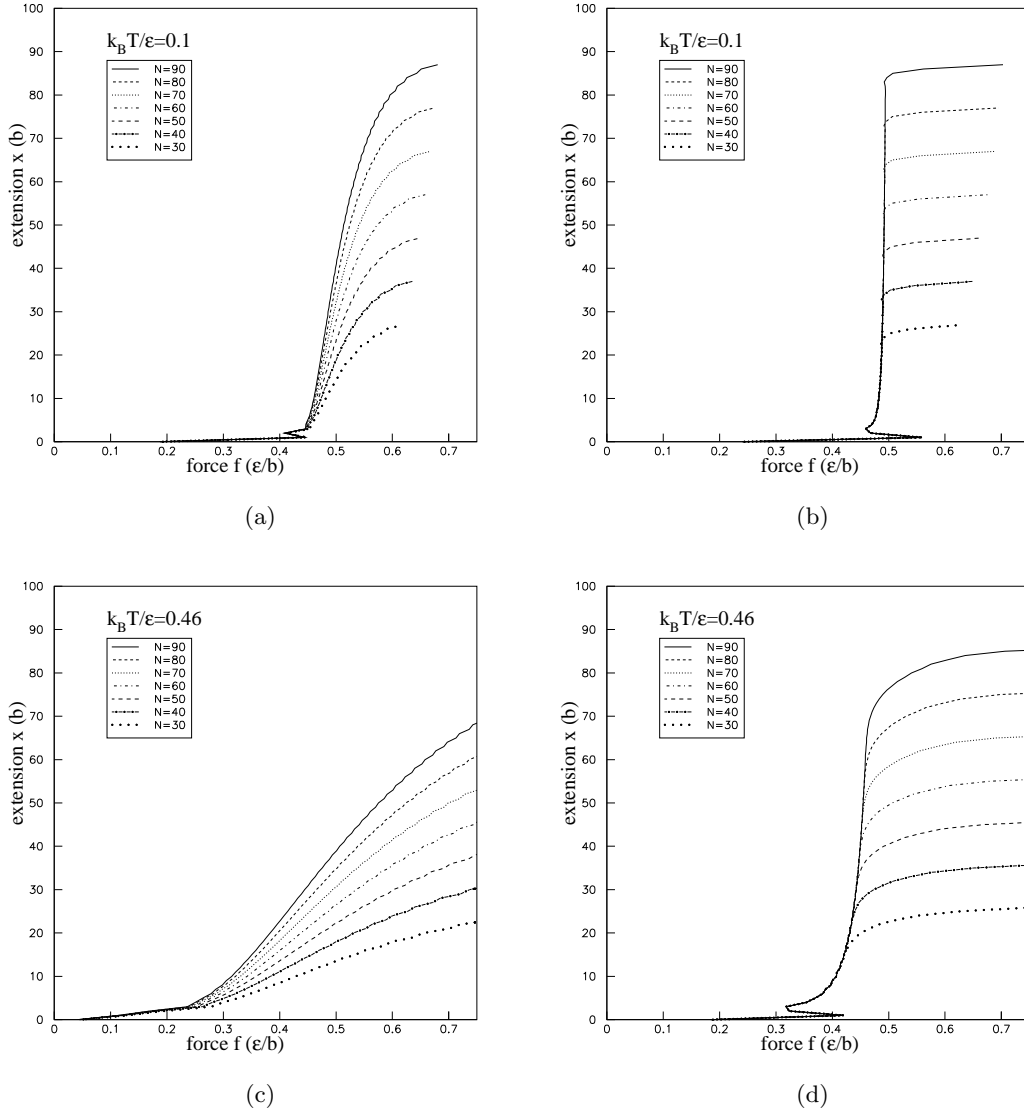


FIG. 7: The FECs of homogeneous chains restricted to secondary structure conformations: (a), (c), and hairpin conformations: (b), (d). To compare with EFCs of constant force ensembles[22], x-coordinate is set to be force f .

locate at two sides of the chain. We did not observe the phenomena for the same chain in constant force ensembles before. To characterize the phenomena quantitatively, we introduce AF $S(L, R)$,

$$S(L, R) = \theta(L - R) \left(1 - \frac{\min(L, R)}{\max(L, R)}\right), \quad (15)$$

where L and R are the number of monomers apart from the middle position to the outmost link of CG region; see Fig. 10, θ is SIGN function, and functions $\min(L, R)$ and $\max(L, R)$ equal the minimum and the maximum value of L and R , respectively. S values of the CGs located completely on the left (right) of middle position are assumed to be +1 (-1), while in conformations containing no contacts, take $S = 0$.

Then define population probability $p(m, s; T)$ as

$$p(m, s; T) = \mathcal{Z}_N(s; T, m) / \mathcal{Z}_N(T; m), \quad (16)$$

where $\mathcal{Z}_N(s; T, m)$ also is the conditional partition function for all the conformations whose AF values are s . Figs. 11(a) and (b) are the distributions of 30-mer homogeneous hairpin chain at temperatures 0.1 and $0.5\epsilon/k_B$. We see that the $p(m, s; T)$ can be divided into four parts, e.g., in the Fig. 11(a): at very small extensions (about smaller than $2b$), the

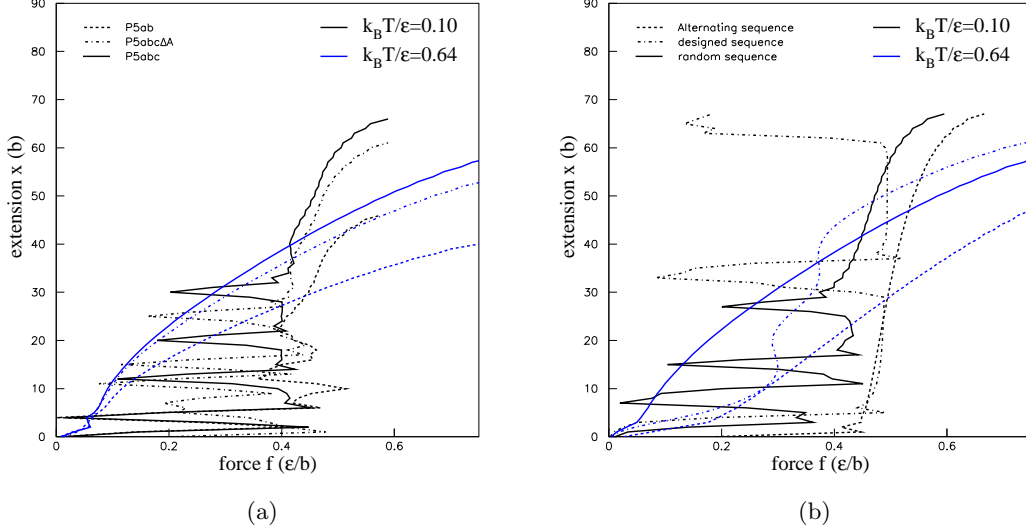


FIG. 8: The FECs of heterogeneous secondary structure chains: (a) the sequences are 49-mer P5ab, 65-mer P5abc Δ A and 69-mer P5abc. (b) 70-mer sequences are random, alternating and designed. Two colors represent FECs at different temperature.

maximum values of the distribution are at $s = 0$, i.e., the CGs of the dominant conformations locate on the middle of the chain according to the definition of AF; when extensions are larger but still smaller some value (about $15b$), the maximum distribution locate at $0 < \pm s < 1$. It means that CG regions stand two side of the chain. Interestingly, these s values stand on two lines ('X' patterns in figures); if increasing extensions further (smaller than $26b$), the s values of the maximum distributions are ± 1 ; finally, distributions will shift to $s = 0$ as extensions reach the full length.

The behaviors of the distribution at the first and third parts can be understandable. As extensions are very small or even vanish, the favorable conformations of the hairpin are those of most contacts. At lower temperatures, say $0.1\epsilon/k_B$, for homogeneous chain, such conformations are forming consecutive contacts: $(0, N), (1, N-1), \dots, (N/2-1, N/2+2)$. Hence, the AF value of the maximum distribution is 0. While extensions is larger enough, or temperatures are higher, if the number of monomers of the CG is smaller than $N/2$, the total number of conformations whose CGs present in two sides must be far larger than that whose CGs stand in the middle of the chain. According to AF definition, the distributions naturally concentrated on $s = \pm 1$; this is only combination result. But why in a range of extensions, the dominant conformations tend to form at two sides of the chain, or AF is neither 0 nor ± 1 , even if their CGs across over the middle position? Considering that contact interactions along the chain is uniform, energy must not be the reason. We believe that the nonuniform EV interactions of the CG regions and two tails with different lengths (see Fig. 4) lead to the tendency: under fixed extension and the same number of CG size, the number of conformations having two tails with lengths l_1 - and l_2 -mer is smaller than the number of conformations having one $(l_1 + l_2)$ -mer tail; or given the same number of tail monomers, the EV effects of CG region are more strong with two tails than with one tail. At temperature $0.1\epsilon/k_B$, given the extension x , because of the most number of contacts encouraged, then the maximum CG size $(N - x)$ -mer is favorable. If supposing one tail existing at left, one easily give the following relation: $s \approx \pm 2x/N = \pm 2\rho$. Comparing it with Fig. 11(a), the formula agree with the pattern very well: the slopes of two lines are about ± 2 . On the other hand, Fig. 11(b) shows that the slopes increase with temperature. In fact, at higher temperature T_h , the maximum CG size is unfavorable for thermal fluctuation. For the same extension, given that L and R values at origin temperature are l and r respectively. Supposing t contacts broken at T_h , then the s -value changes from $1 - r/l$ to $1 - (r - t)/(l - t)$. Apparently, AF is the increasing function of t , while t also be an increasing function of temperature. As a comparison, we partially cancel EV interactions: when one length of two tails is larger than some value, here $5b$ is taken, the interactions will be screened. The distribution of 30-mer chain is computed again under this the requirement; see Fig. 12(a). The maximum values of distribution at a fixed extension are not located on a unique s , or CGs distribute on the chain uniformly. Because the lines with slopes ± 2 represent the maximum asymmetry at temperature $0.1\epsilon/k_B$, other AF values must stand between them (see "butterfly" pattern in Fig. 12(a)).

It may provide useful insights into the force stretching problem using asymmetric concept. Define $p(f, s; T) = \mathcal{Q}_N(f, s; T) / \mathcal{Q}_N(T; f)$, where conditional partition function $\mathcal{Q}_N(f, s; T)$ is for all conformations whose asymmetric factor is s , and $\mathcal{Q}_N(T, F)$ is full partition function[22]. Fig. 12(b) is the diagram of $p(f, s; 0.1)$ of 30-mer homogeneous

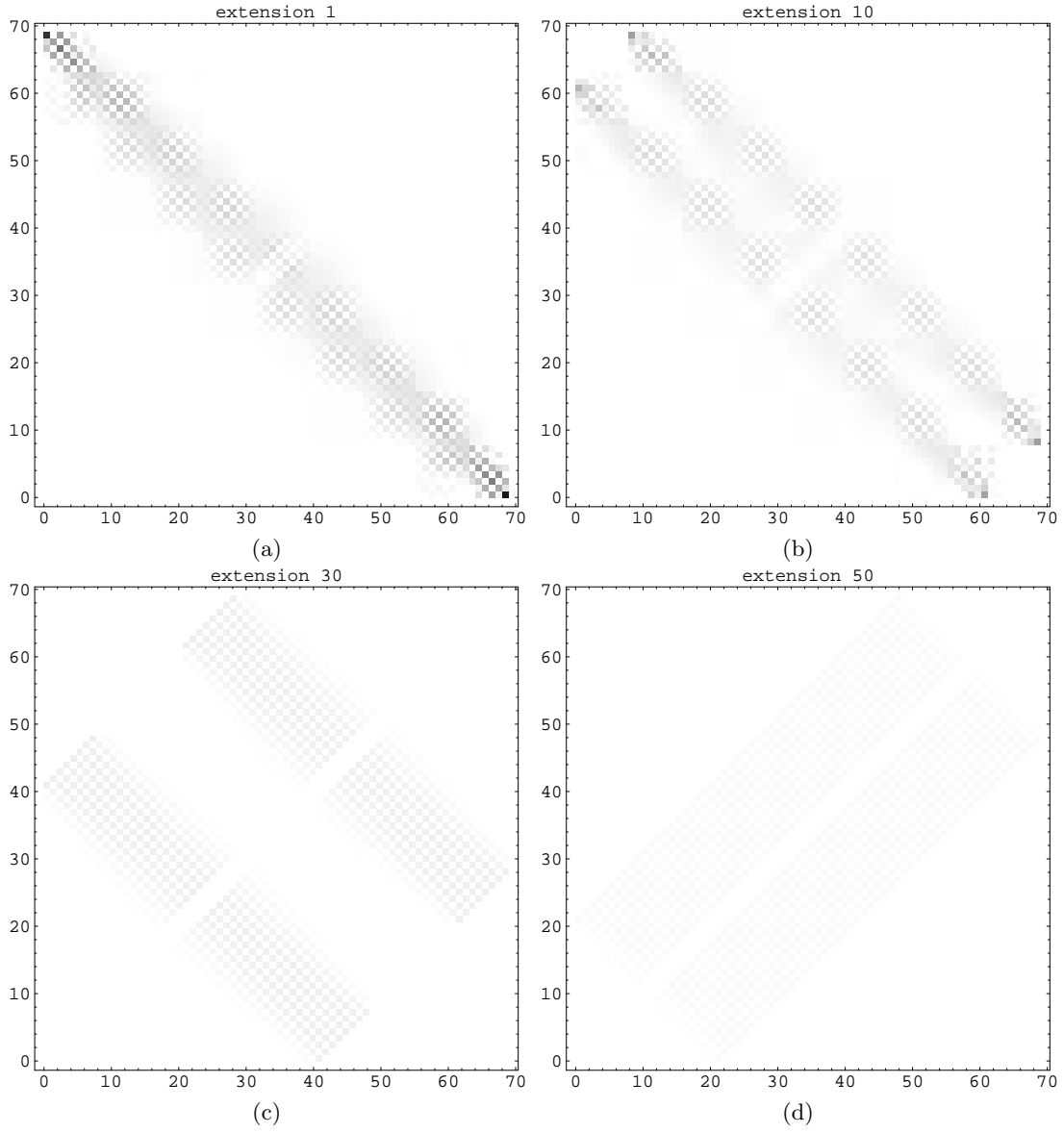


FIG. 9: The density diagrams for contact probability $p(i, j; T, m)$ of a 70-mer homogeneous chain of hairpin conformations at different extensions 1, 10, 30 and 50. Here temperature is $0.1\epsilon/k_B$. When extensions are smaller, such as in (b) and (c), nonzero contacts populate two sides of, instead of along the catercorner of the diagrams.

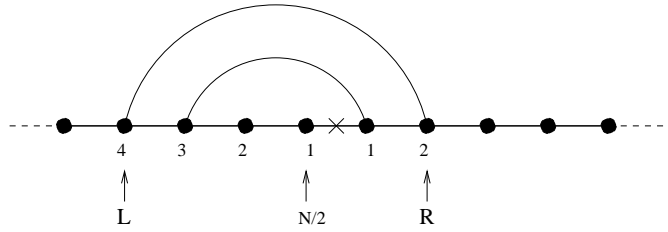


FIG. 10: Sketch of the AF S definition. L and R are the number of monomers apart from the middle position ('x' symbol) of the chain to the outmost link of CG region. Here even value of N is considered for simplicity.

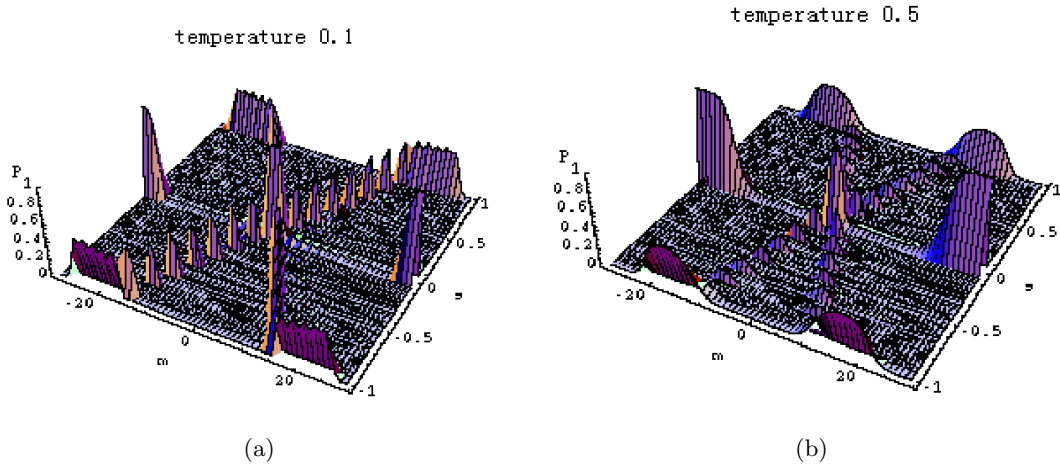


FIG. 11: The population probabilities $p(m, s; T)$ for 30-mer homogeneous chain of hairpin conformations. Temperatures are 0.1 and $0.5\epsilon/k_B$. Apparent ‘X’ patterns can be observed in figures, which shows that CG regions of dominant conformations at these extensions tend to form at two sides of the chain.

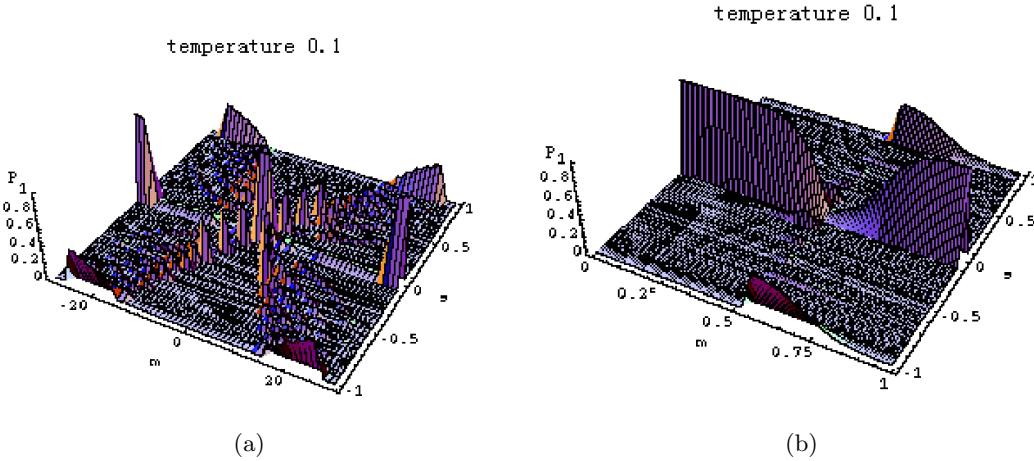


FIG. 12: (a) The population probabilities $p(m, s; T)$ for 30-mer homogeneous chain, where EV interactions between CG regions and two tails are considered partially. the ‘X’ in Fig. 11 transforms into “butterfly”. (b) The population probabilities $p(f, s; T)$ at temperature $0.1\epsilon/k_B$, where forces are in unit ϵ/b . The extent of $s = \pm 1$ becomes narrow as value of N increases, since EFCs of the hairpin conformations have first-like behavior.

hairpin chain. The $p(f, s; T)$ is very different from $p(x, s; T)$, e.g., the AF values of the former change from 0 to ± 1 , and reenter into 0 in narrow force ranges, whereas for the latter, the changes of the AF are continuous and slowly. At temperature $0.1\epsilon/k_B$, when forces are smaller than $0.48\epsilon/b$, states having the most number of contacts are favorable, which means most possibility values of AF are 0. Because of higher cooperativity in hairpin conformations, the structures are collapsed in small force range as $f > 0.48\epsilon/b$ [22]. It means AF vanishes again. The temporary $s = \pm 1$ should be the results of finite chain length.

C. Force flipping phenomena

Finally, we explore the force dependence on temperatures as fixed extension. The studies are related with the re-entering transition studied in unzipping dsDNA[19, 20]. The transition means that if one fixes external force at a value in a finite range and decreases temperature, beginning with stretched state, dsDNA will first collapse to a globular state; while temperature is lowered further, dsDNA will re-enter stretched state again. We have discussed the phenomenon in constant force stretched homogeneous chains of hairpin and secondary structure conformations in Ref. [22]: the re-entering transition only presents in hairpin case. To our knowledge, the conjugated phenomena of re-entering transitions in constant extension ensembles are not investigated before. Our model can be used to check

the problem by numerical computing FTCs of homogeneous chains of hairpin and secondary structure conformations, respectively. The results of 25-mer chains are shown in Fig. 13: force flipping (the arrow therein) presents at lower temperature in hairpin conformations, but is not observed in secondary structure conformations. We believe that the flipping just corresponds to re-entering transitions in constant force ensembles. This results could be explained qualitatively. First, the temperatures of flipping and re-entering transitions are almost the same, i.e., about $0.23\varepsilon/k_B$ [22]. Second, like the absence of flipping in secondary structures, re-entering transitions of this conformations are not observed in constant force ensembles. Finally, because of the equivalence of constant extension and constant force ensembles of homogeneous chains, the FTCs at fixed extensions could be derived from the extension-temperature curves (ETCs) at fixed force. In the fixed force ensembles, if there is a dip at lower temperature T_r in the ETC of a given force, then at least two temperatures located at two sides of T_r correspond to the same extensions x_o . If the dip rises as the force increasing, the extension x_o will have a series of temperatures standing in two sides T_r , which will form a convex in FTC at T_r . The dips in ETCs of hairpin conformations do have such characteristics[22]. We can use the same approach to understand FTCs behaviors of secondary structure conformations.

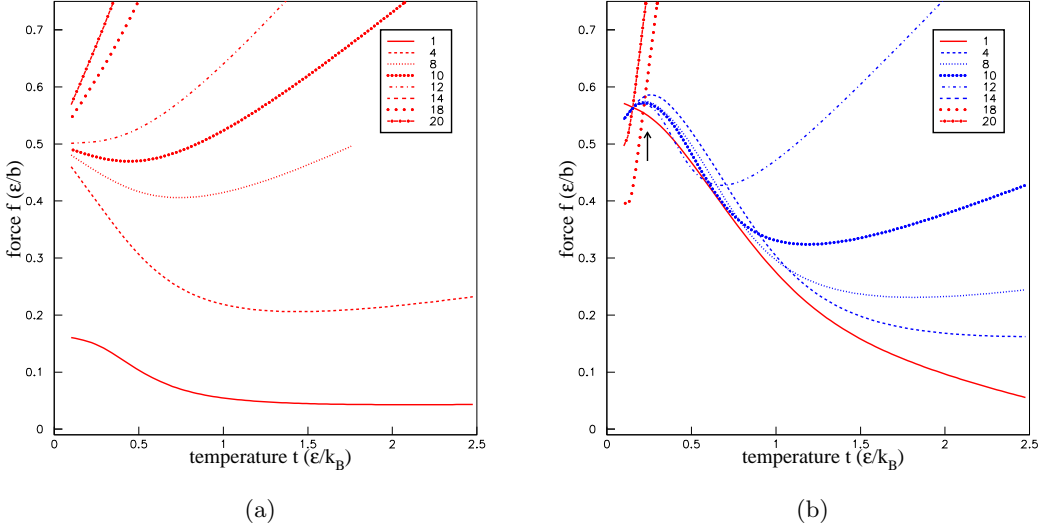


FIG. 13: The TFCs of 25-mer chains of secondary structure (a) and hairpin conformations (b) at different fixed extensions, where the sequences are homogeneous. Arrow in (b) points out the convex, which demonstrates the appearance of force-flipping transition.

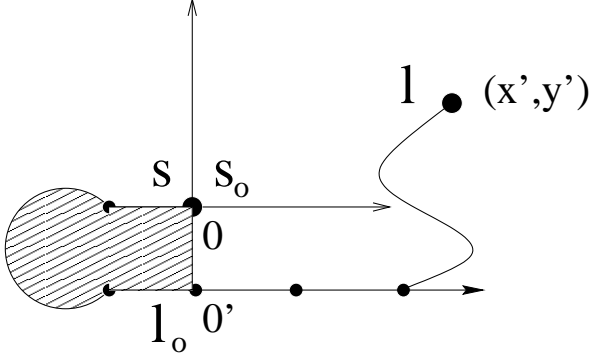
V. SUMMARY

In this paper, we propose a statistical model of constant extension ensembles of double-stranded chain molecules. Unlike several theoretical models proposed previously, specific monomers sequence and EV interaction are exactly included. Using the model, we investigate how FECs depend on chain length, sequence, and structure. In addition, the model can relate FECs with molecule structure directly. The structures of hairpin conformations reveal that CG regions tend to form at two sides of chains as the extensions are in some range. This unexpected phenomena have never been reported before. Through introducing AF and analyzing in detail, we contribute the phenomena to EV interactions between CG regions and tails. We also explore the conjugated transitions of re-entering in constant extension ensembles, the force-flipping phenomena, which only present in hairpin conformations. Because our aim in this paper is to illustrate, the model is largely simplified, e.g., the chain is restricted on 2D lattice, chain stiffness (bending) and elasticity are neglected, and no stacking interaction is involved. However, our results still give many important physical information, especially the importance of the long-range EV interaction. In future work, we will replace the projection extension by real EEDs. It is interesting to see whether the position tendency of CGs is still observed.

Acknowledgments

We are grateful to Dr. Shi-jie Chen, and Prof. H.-W. Peng for much useful discussion.

APPENDIX A: CALCULATING EXTENSIONS OF THE HAIRPIN CONFORMATIONS



T	Δ	T	Δ
E	x'	M_x	x'
C_4^1	$-y'+1$	M_y	$-x'$
C_4^2	$-x'$	σ_v	$y'-1$
C_4^3	$y'-1$	σ_v	$-y'+1$

FIG. 14: One class of conformations for the 2nd tail (l_o, l) and closed graph (s_o, l_o) containing outmost type 1 link, where the tail type is stiff and extends upward [17]. The end l located at (x', y') on frame O' is translated to point $(x', y' - 1)$ on frame O , and the corresponding extension Δ is x' . We can distribute the conformation to lattice plane by eight square symmetry transformations (see Fig. 4). The extension Δ s are tabulated respectively, where the character ‘‘T’’ represents transformation elements.

For hairpin conformations, the conformations of tails are determined by two factors: the outermost link type and the length of closed graph. To account for EV interactions, the tails have been classified into two types, stiff (s) and flex (f)[17]. Correspondingly, the number of conformations is $n^{t_i}(N_i)$, where t_i (s or f) are the type of i th (1st or 2nd) tail with length N_i , or N_i -step OSAW. In order to calculate extensions of the whole chain, we introduce additional definitions: $n_x^{t_i}(N_i; m)$, the number of conformations for i th OSAW of type t_i whose final x coordinates are m ; and $n_y^{t_i}(N_i; m)$ is similar except y coordinate. It is ease to find $n^{t_i}(N_i) = \sum_m n_x^{t_i}(N_i; m) = \sum_m n_y^{t_i}(N_i; m)$. Here we illustrate the calculation of the simplest diagonal matrix element $\omega(l, l_0; s_0, s|\Delta)_{11}$, where the outmost link is of type 1 and $s = s_0, l \neq l_0$. Because other more general cases have more cumbersome formula, we are not listed them in the present paper.

There are six classes of possible conformations for the simplest CG-tail complexes[17]. In Fig. 14, we show one of them. The length of the 2nd tail then is $N_2 = l - l_o$. Since the length of CG also affects EV interactions, we distinguish different CG sizes.

(1) $l_o - s_o = 3$. All six classes of conformations are viable. Therefore,

$$\begin{aligned}
 \omega(l, l_0; s_0, s|\Delta)_{11} = & 2 [n_y^{f_2}(N_2; \Delta) + n_y^{f_2}(N_2; -\Delta) + n_y^{f_2}(N_2; \Delta - 1) + n_y^{f_2}(N_2; -(\Delta + 1)) \\
 & + n_x^{f_2}(N_2; \Delta) + n_x^{f_2}(N_2; -\Delta) + n_x^{f_2}(N_2; \Delta - 1) + n_x^{f_2}(N_2; -(\Delta + 1)) \\
 & + 2n_y^{s_2}(N_2; \Delta) + 2n_y^{s_2}(N_2; -\Delta) + n_y^{s_2}(N_2; \Delta - 1) + n_y^{s_2}(N_2; -(\Delta + 1)) \\
 & + n_y^{s_2}(N_2, \Delta + 1) + n_y^{s_2}(N_2; -(\Delta - 1)) \\
 & + 2(n_x^{s_2}(N, \Delta) + n_x^{s_2}(N, -\Delta) + n_x^{s_2}(N, \Delta - 1) + n_x^{s_2}(N, -(\Delta + 1))) \\
 & - (2\delta_{0,\Delta} + \delta_{1,\Delta} + \delta_{-1,\Delta} + \delta_{N_2,\Delta} + \delta_{-N_2,\Delta} + \delta_{N_2+1,\Delta} + \delta_{-(N_2+1),\Delta})], \quad (A1)
 \end{aligned}$$

where coefficient 2 is *degeneracy degree* along projection, the negative part is to eliminate the straight tail conformations, which are counted repeatedly.

(2) $l_o - s_o > 3$. There are five classes of conformations are involved. We have

$$\begin{aligned}
 \omega(l, l_0; s_0, s|\Delta)_{11} = & 2 [n_y^{f_2}(N_2; \Delta) + n_y^{f_2}(N_2; -\Delta) + n_y^{f_2}(N_2; \Delta - 1) + n_y^{f_2}(N_2; -(\Delta + 1)) \\
 & + n_x^{f_2}(N_2; \Delta) + n_x^{f_2}(N_2; -\Delta) + n_x^{f_2}(N_2; \Delta - 1) + n_x^{f_2}(N_2; -(\Delta + 1)) \\
 & + n_y^{s_2}(N_2; \Delta) + n_y^{s_2}(N_2; -\Delta) + n_y^{s_2}(N_2; \Delta - 1) + n_y^{s_2}(N_2; -(\Delta + 1)) \\
 & + n_y^{s_2}(N_2, \Delta + 1) + n_y^{s_2}(N_2; -(\Delta - 1)) \\
 & + 2(n_x^{s_2}(N, \Delta) + n_x^{s_2}(N, -\Delta)) + n_x^{s_2}(N, \Delta - 1) + n_x^{s_2}(N, -(\Delta + 1)) \\
 & - (\delta_{1,\Delta} + \delta_{-1,\Delta} + \delta_{N_2,\Delta} + \delta_{-N_2,\Delta})].
 \end{aligned} \tag{A2}$$

-
- [1] S. B. Smith, Y. J. Cui, and C. Bustamante, *Science* **271**, 795 (1996).
[2] B. Maier, D. Bensimon, and V. Croquette, *Proc. Natl. Acad. Sci. USA* **97**, 12002 (2000).
[3] J. Zlatanova, S. M. Lindsay, and S. H. Leuba, *Prog. Biophys. Mol. Biol.* **74**, 37 (2000).
[4] M. Rief, M. Gautel, F. Oesterhelt, J. M. Fernandez, and H. E. Gaub, *Science* **276**, 1109 (1997).
[5] K. Visscher, M. J. Schnitzer, and S. M. Block, *Nature(London)* **400**, 184 (1999).
[6] U. Bockelmann, b. Essevez-Roulet, V. Viasnoff, and F. Heslot, *Biophys. J.* **82**, 1537 (2002).
[7] J. Liphardt, B. Onoa, S.B. Smith, I.J. Tinoco, and C. Bustamante, *Science* **292**, 733 (2001).
[8] M. Rief, H. Clausen-Schaumann, and H. E. Gaub, *Nature struct. Biol.* **6**, 346 (1997).
[9] J. F. Marko and E. D. Siggia, *Macromolecules* **28**, 8759 (1995).
[10] H.-J. Zhou, Y. Zhang, and Z.-C. Ou-Yang, *Phys. Rev. Lett.* **114**, 8694 (2001).
[11] A. Montanari and M. Mézard, *Phys. Rev. Lett.* **86**, 2178 (2001).
[12] D. K. Lubensky and D. R. Nelson, *Phys. Rev. E* **65**, 031917 (2002), and references therein.
[13] U. Gerland, R. Bundshuh and T. Hwa, *Biophys. J.* **81**, 1324 (2001).
[14] J. T. Titantah, *Phys. Rev. A* **60**, 7010 (1999).
[15] S. M. Bhattacharjee and D. Marenduzzo, *J. Phys. A: Math. Gen.***35**, L349 (2002)
[16] S.-J. Chen and K. A. Dill, *J. Chem. Phys.* **103**, 5802 (1995).
[17] S.-J. Chen and K. A. Dill, *J. Chem. Phys.* **109**, 4602 (1998).
[18] M.-N. Dessinges, B. Maier, Y. Zhang, M. Peliti, D. Bensimon and V. Croquette, *Phys. Rev. Lett.* **89**, 248102 (2002).
[19] D. Marenduzzo *et al.*, *Phys. Rev. Lett.* **88**, 028102 (2002).
[20] E. Orlandini *et al.*, *J. Phys. A* **34**, L751 (2001), and references therein.
[21] V. Munoz, P. A. Thompson, J. Hofrichter, and W. A. Eaton, *Nature(London)* **390**, 196 (1997).
[22] F. Liu, L.R. Dai and Z.-C. Ou-Yang, (2002), cond-mat/0212268.
[23] M. E. Fisher, *J. Chem. Phys.* **44**, 616 (1966).